RESONANCE AMONG WAVES, CURRENT, AND RIPPLED BOTTOMS IN COASTAL ZONES – FLOW FIELD RESPONSE UNDER INTENSIVE RESONANCE

Jun Fan[1,2], Aifeng Tao[1,2], Jinhai Zheng[1,2]

Due to the coexistence of free-surface waves, tidal & nearshore currents, as well as the continuous submarine sandbars in coastal and estuarial areas, the hydrodynamics processes involving wave, current, and rippled bottoms have drawn increasing attention. The phenomenon of the new wave component excitation (i.e. upstream-propagating waves), indicates the resonant interaction among wave, current, and rippled bottoms. Under the condition of intensive wave excitation induced by resonance, the flow field responses were observed by the flume experiment. Different tracing methods were applied to reveal the flow pattern above the rippled bottoms. The vortex shedding process presents the synchronous behavior with the free-surface oscillation under the flow condition corresponding to the excitation of upstream-propagating waves. Besides, the flow field responses under the flow velocities which are below and above the wave excitation domain are also compared with the situation within the wave excitation domain.

Keywords: coastal hydrodynamics; resonant interaction; undulating bottoms; flow field observation

INTRODUCTION

In many coastal and estuarial areas, large-scale continuous submarine sandbars have been measured in the past few decades. Besides, strong tidal and nearshore currents also exist in these regions. Due to the co-existence of free-surface water waves, ambient flow, and continuous submarine sandbars, the hydrodynamic characteristics especially the interaction effects among these elements are very complex (Raj and Guha 2019, Choi *et al*. 2021, Yih 1976, McHugh 1992). Previously, the interactions above were usually studied separately in coastal hydrodynamics, i.e., Bragg resonance between water waves and rippled bottoms (Davies and Heathershaw 1984, Mei 1985, Liu and Yue 1998), stationary waves for steady flow over rippled patch (Kennedy 1963, Mei 1969, Mizumura 1995), as well as the wave-current interaction (Mei *et al*. 2005).

In recent years, a special water wave phenomenon was studied in detail and called upstream-propagating waves (Kyotoh and Fukushima 1997, Fan *et al*. 2014, 2016, 2021, 2022). It is generated on the free surface by flow over rippled bottoms. The study for this specific wave component will provide new insights into wave-current-bottom resonant interaction. We have performed a series of flume experiments, in which the different flow depths and flow velocities were adjusted above the rippled bottoms. Under the specific range of flow conditions, the free-surface waves are induced to propagate upstream continuously. During the wave generation process, the detailed wave elements are observed as monochromatic waves as shown below. At the same time, intensive free-surface oscillations occurred above the rippled patch.

Besides, perturbation analysis was made to illustrate its generation mechanism. This wave is induced by a special triad resonance involving free-surface disturbance waves, flow, and rippled patches. Its wave amplitude will be enlarged obviously near a critical flow condition which corresponds to the wave energy blocking to form the obvious upstream-propagating waves. The wave amplitudes' temporal and spatial evolution properties have been derived and identified (Fan *et al*. 2021, 2022).

However, the flow field features during the wave generation process are still unknown and need to be considered due to the intensive free-surface oscillation above the rippled patch. In this study, the flow field responses observed by tracing methods during the flume experiment under the generation conditions of upstream-propagating waves are stated. It will provide intuitive evidence of the flow field variation under the intensive excitation process of new wave components induced by resonance among free-surface waves, ambient current, and rippled bottoms.

The remainder of this paper is organized as follows. The basic information of the flume experiments is briefly stated in Section 2. The flow field response shown by tracing methods under intensive resonance is presented in Section 3. Then Section 4 contains discussions and conclusions.

BRIEF INFOMATION OF THE FLUME EXPERIMENT

The experiment was conducted in the wave-current flume with a total length of 51 m, for which, the side walls are constructed from glass. Beneath the flume, the water pipes and pumps were installed to create a steady flow with adjustable velocity. The rippled patch was fixed in the flume bottom, which is partially embedded in the flume bottom to keep the average height position of the rippled bottom coinciding with the flat bottom of the flume. The wavelength L_b of the fixed rippled bottom topography

[1] Key Laboratory of Ministry of Education for Coastal Disaster and Protection, Hohai University, Nanjing, China, 210024.
[2] College of Harbour, Coastal and Offshore Engineering, Hohai University, Nanjing, China, 210024.

is 0.24 m, and its amplitude A_b is 0.04 m. Eight sinusoidal rippled undulation bottoms were installed, and the total length of the rippled bottom section was 1.80 m. During the flume experiment, the wave paddle was always closed and the flow conditions (water depth h and flow velocity presented as Froude number F) were adjusted for different cases. The detailed information of the flume apparatus and case arrangement could be referred to the previous publications (Fan *et al*. 2021).

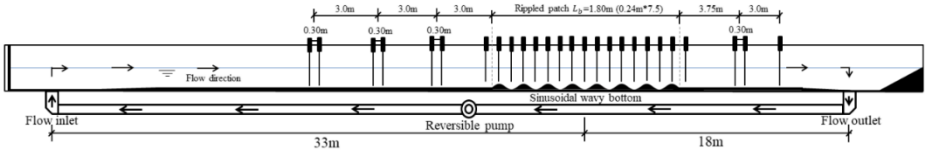

Figure 1. Sketch of the flume experiment of the generation of upstream-propagating waves (Fan *et al*. 2021)

Specifically, to observe the flow field responses above the rippled bottoms during the excitation process of the upstream-propagating waves, two tracing methods were applied during the flow field observation process.

The first method is the laser flow field tracing. The flow and bottom parameters corresponding to the cases with the intensive excitation of upstream-propagating waves include the bottom steepness of 0.333 (the bottom wave height being 8.0 cm), the relative water depth h/L_b of 0.8 (the actual average water depth being 19.2 cm), and the Froude number F=0.24. The self-made laser flow field tracing facilities were made to visualize the flow field during the generation process of the upstream-propagating waves. In detail, a laser sheet light source generator was installed above the free surface at the position of the sinusoidal rippled bottoms. The output power of the laser was 30 mW. A semiconductor electrically excited continuous laser was adopted, which emitted green laser light with a wavelength of 532 nm and outputted a sheet laser light source in the direction of the underwater flow field through a glass cylindrical mirror. Meanwhile, the surface of the wooden rippled bottoms at the bottom of the water was painted black to reduce the light scattering of the laser. During the experiment, an underwater elbow pipe was set at approximately 50 cm upstream of the first wave crest of the rippled patch. Then, the suspension of titanium dioxide or aluminum oxide was released through a large-capacity syringe for tracing purposes. The Canon EOS 5D Mark III high-definition camera was used to capture the movement characteristics of the suspension between the first and second bottom ripples, and also between the second and third bottom ripples of the sinusoidal patch after the release of the suspension.

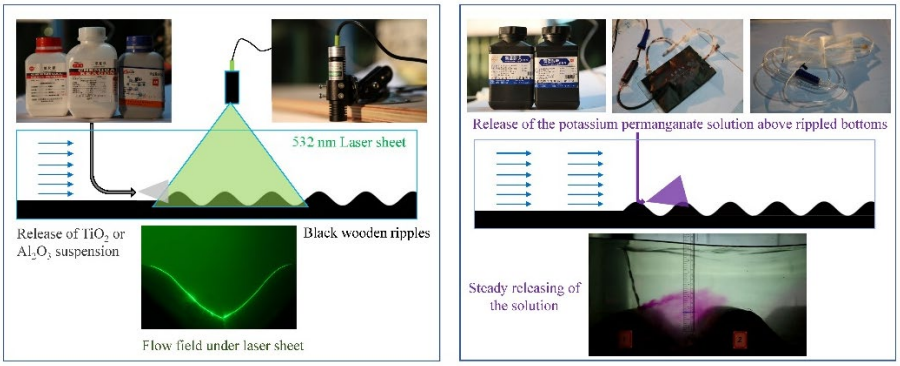

Figure 2. Sketch of the tracing methods of the flow field above the rippled bottoms

The second method is the potassium permanganate solution flow field tracing. Regarding the flow field response under different flow velocity conditions, this attempt was made to use the medical intravenous infusion set to continuously and slowly inject the saturated potassium permanganate solution into the flow fields at different positions near the rippled bottoms (usually at the first and second wave crests) through a syringe, to observe the flow motion through the tracer solution. The cases' parameters include the wave steepness of 0.333 (the rippled bottom's wave height being 8.0 cm), relative water depth of 0.8 (the actual average water depth being 19.2 cm), and Froude numbers F of 0.17, 0.24, and 0.31 respectively. Then the high-definition camera was used to shoot the flow patterns and motion processes after the release of the tracer solution.

FLOW FIELD RESPONSE UNDER INTENSIVE RESONANCE

Based on the tracing methods above, the flow field responses were observed under the generation condition of upstream-propagating waves as the intensive resonance among free-surface waves, ambient current, and rippled bottoms. Besides, the flow field responses under the flow velocity values which are below and above the wave excitation range are illustrated for further comparison.

Laser sheet tracing of the flow field

Qualitative observations of the flow field characteristics were made through the constructed simple laser sheet light source observation equipment above the rippled bottoms when the upstream-propagating waves were generated. For the flow field observation experiment, the condition with the ripped bottom steepness of 0.333, a relative water depth of 0.8, and a Froude number of 0.24 was selected. For the flow field characteristics between the first and second bottom wave crests, the titanium dioxide suspension was uniformly and slowly injected from the upstream side, and the green laser sheet light source set above the rippled patch was used for tracing. Fig. 3 shows the continuous screenshots of the flow field tracing video, which includes the flow field situations at 15 observation moments (numbered from 01 to 15). The time interval corresponding to each picture is 1/23 s, and the left wave crest in each figure is the first wave crest of the rippled patch.

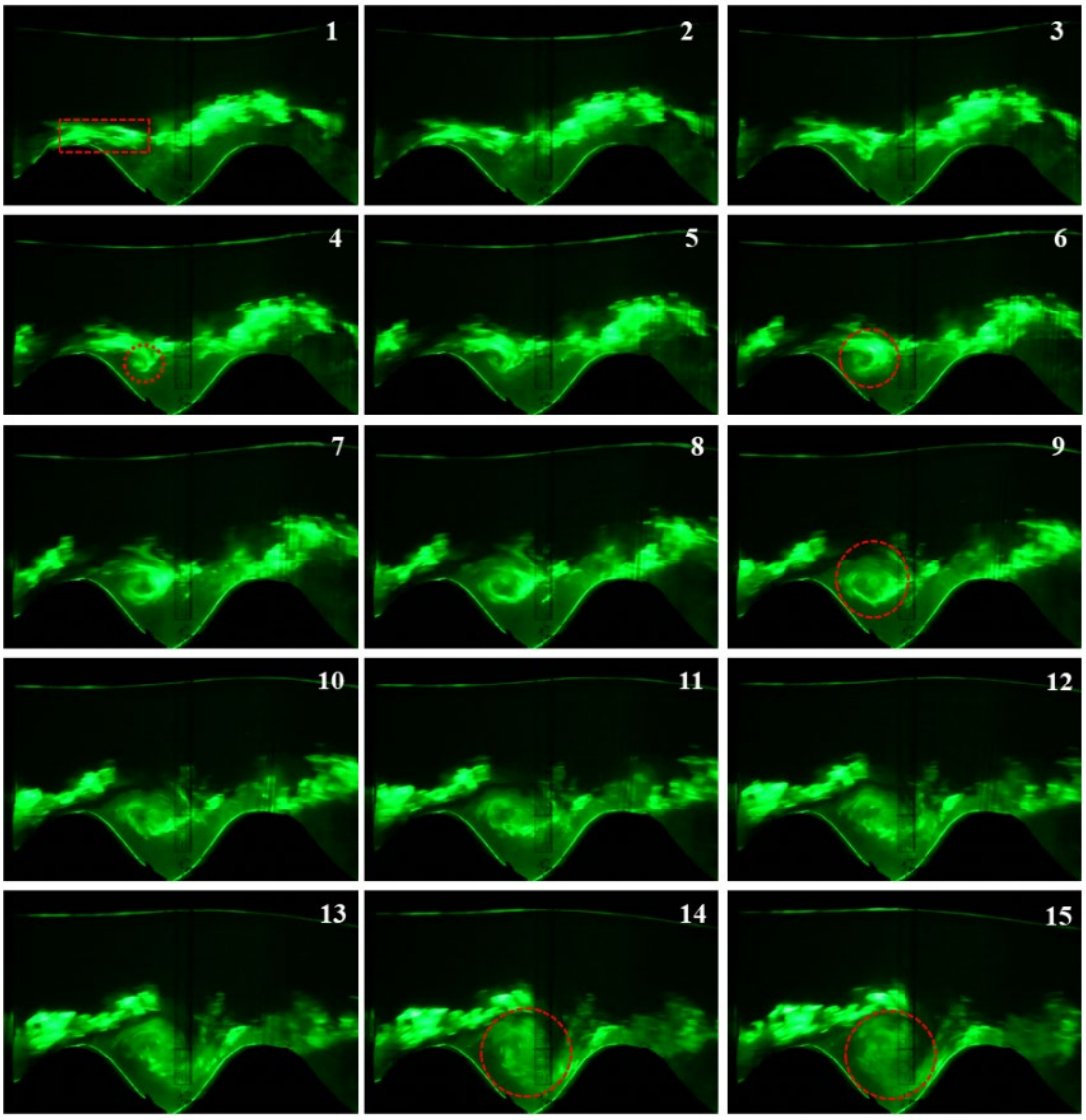

Figure 3. The time variation process of the vortex structure observed through laser flow field tracing (with the bottom wave steepness of 0.333, the relative water depth of 0.8, and the Froude number of 0.24).

At moment 01 in Fig. 3, the high-brightness water body marked by the red dashed square box flows through the position of the first crest of the rippled patch, and during its movement downstream (moments 02 - 03), there is a slight drop in the corresponding water body position. In the figure at moment 04, the high-brightness water body moves to the position of the red dashed circle in the picture and begins to show the rotating motion state, and the range of motion gradually increases, forming an obvious vortex structure. After that, the motion state of the high-brightness water body with the vortex structure begins to develop, and the volume of the vortex structure continues to increase, as shown by the red dashed circles in the figures at moments 06 and 09. In addition, as the volume of the vortex structure increases, its position also moves towards the center of the trough downstream of the wave crest, as shown in the figures corresponding to moments 14 and 15, and the gradually expanding red dashed circle represents the water body after the expansion of the vortex structure volume.

In the flow field observation under the same experimental case conditions, in addition to observing the vortex structure on the downstream side of the rippled bottom's crest, there is also an obvious backflow phenomenon near the wall surface on the downstream side of the bottom wave crest, as shown in Fig. 4. The time interval corresponding to the 15 consecutive screenshots of the flow field video in the figure is also 1/23 s, and the observation position is the same as that in Fig. 3.

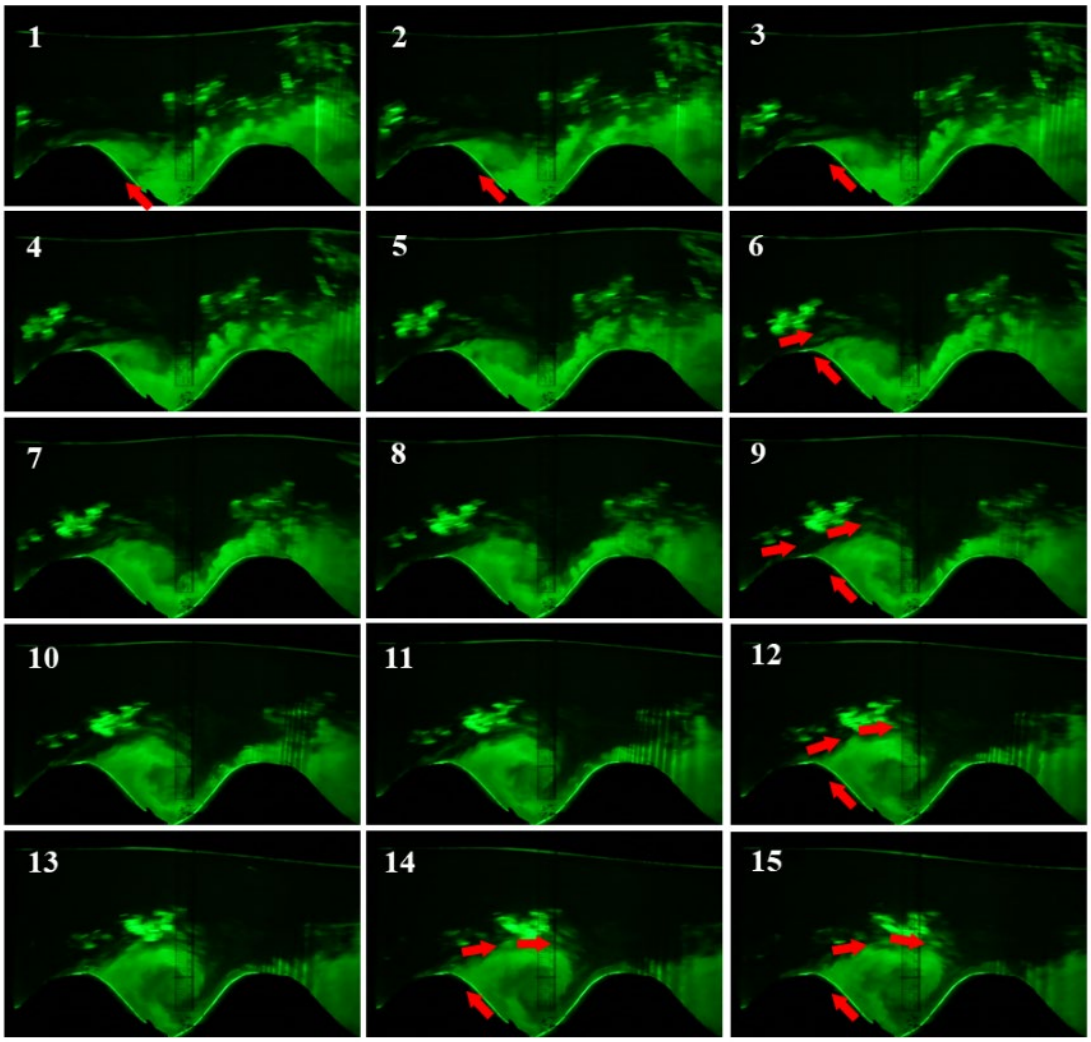

Figure 4. The characteristics of the backflow area and vortex motion observed through laser flow field tracing (with the bottom wave steepness of 0.333, the relative water depth of 0.8, and the Froude number of 0.24).

It can be observed from moments 01 - 06 in Fig. 4 that there is an obvious backflow phenomenon on the downstream side (leeward side) of the first crest of the rippled bottoms, as indicated by the red arrows in the corresponding figures. Meanwhile, at the top of the backflow area on the downstream side

of the first bottom wave crest position, boundary layer separation caused by the adverse pressure gradient was observed, and its separation point is located near the wall surface on the downstream side of the bottom wave crest, and the flow field on the downstream side of the separation point shows the characteristics of a separation area with an obvious vortex structure.

Furthermore, when the upstream-propagating waves are generated, the motion process of the vortex water body structure caused by the boundary layer separation shows an obvious periodicity. Specifically, an obvious backflow feature appears near the wall surface on the downstream side of the first crest of the rippled bottom, and at the same time, vortex structures are periodically triggered. Moreover, the frequency of vortex generation caused by the boundary layer separation is consistent with the frequency of the upstream-propagating waves on the free water surface above the rippled bottoms. In addition, the periodic boundary layer separation and the subsequent vortex shedding phenomenon are related to the periodic water level change above the bottom crest of the rippled patch. Whenever the water level above the position of the boundary layer separation point starts to rise from the trough of the free-surface wave, the vortex structure is shed on the downstream side of the crest of the rippled bottom.

Regarding the overall motion and change process of the water body with the vortex structure, as shown in Fig. 5, the time interval of the flow fields at each moment (numbered from 01 to 27), the observation position, and the experimental case conditions are the same as those mentioned above. It can be seen from the instantaneous flow field diagrams corresponding to moments 01 - 10 in Fig. 5 that the water body with the vortex structure is generated after the separation point on the downstream side of the bottom wave crest and moves to the trough position on the downstream side of the bottom wave crest, accompanied by the gradual growth of its size. At moments 11 - 15, when the water body with the vortex structure moves to the center position of the bottom trough, the structural size of the water body also reaches its maximum and presents a relatively regular shape (approximately circular). During the period from moments 16 - 21, after the vortex water body has fully grown at the bottom trough position, it then moves downstream. Since this part of the water body is squeezed by the crest of rippled bottoms on its downstream side during the flow process moving downstream, the vortex structure no longer maintains a regular circular shape but becomes elongated due to the rippled patch's squeeze. Through the flow field situations at moments 22 - 27, it can be observed that the deformed vortex structure water body continues to move downstream, but at this time, its horizontal position begins to rise along the slope (windward side) of the bottom wave crest on the downstream side, and finally, the water body with the vortex structure rises above the crest position of the rippled bottoms on the downstream side.

Regarding the relationship between the overall motion and change process of the vortex water body structure and the water surface fluctuation situation, certain patterns can also be observed from Fig. 5 (the white arrows in the figure indicate the water level change trend of the free water surface fluctuation, the red arrows indicate the motion direction of the vortex water body, and the red dashed lines indicate the approximate outline of the vortex water body). When the free water surface trough of the upstream-propagating wave is located above the position of the rippled bottoms' crest (as shown at moments 1-3), an obvious boundary layer separation occurs in the water body immediately downstream of the bottom wave crest and a rapidly rotating vortex structure water body is formed (the shedding of the vortex structure occurs). When the water level at the position of the rippled bottoms' crest begins to gradually rise (during the process of the free-surface wave crest of the upstream-propagating waves moving towards this position), the vortex water body generated due to the boundary layer separation starts to move downstream after its formation, and the size of the vortex structure is also constantly increasing. When the free-surface wave crest shape of the upstream-propagating wave moves to the position above the rippled bottoms' trough, the vortex structure also moves to the vicinity of the rippled bottoms' trough position. As the vortex water body continues to move downstream, accompanied by the diffusion of the water body structure and the deformation of the water body structure caused by the squeeze of another bottom wave crest on its downstream side, when the dissipating vortex water body moves above another bottom wave crest position on the downstream side of the trough, the wave crest of the upstream-propagating wave is also located above the position of the vortex tracing water body at this time.

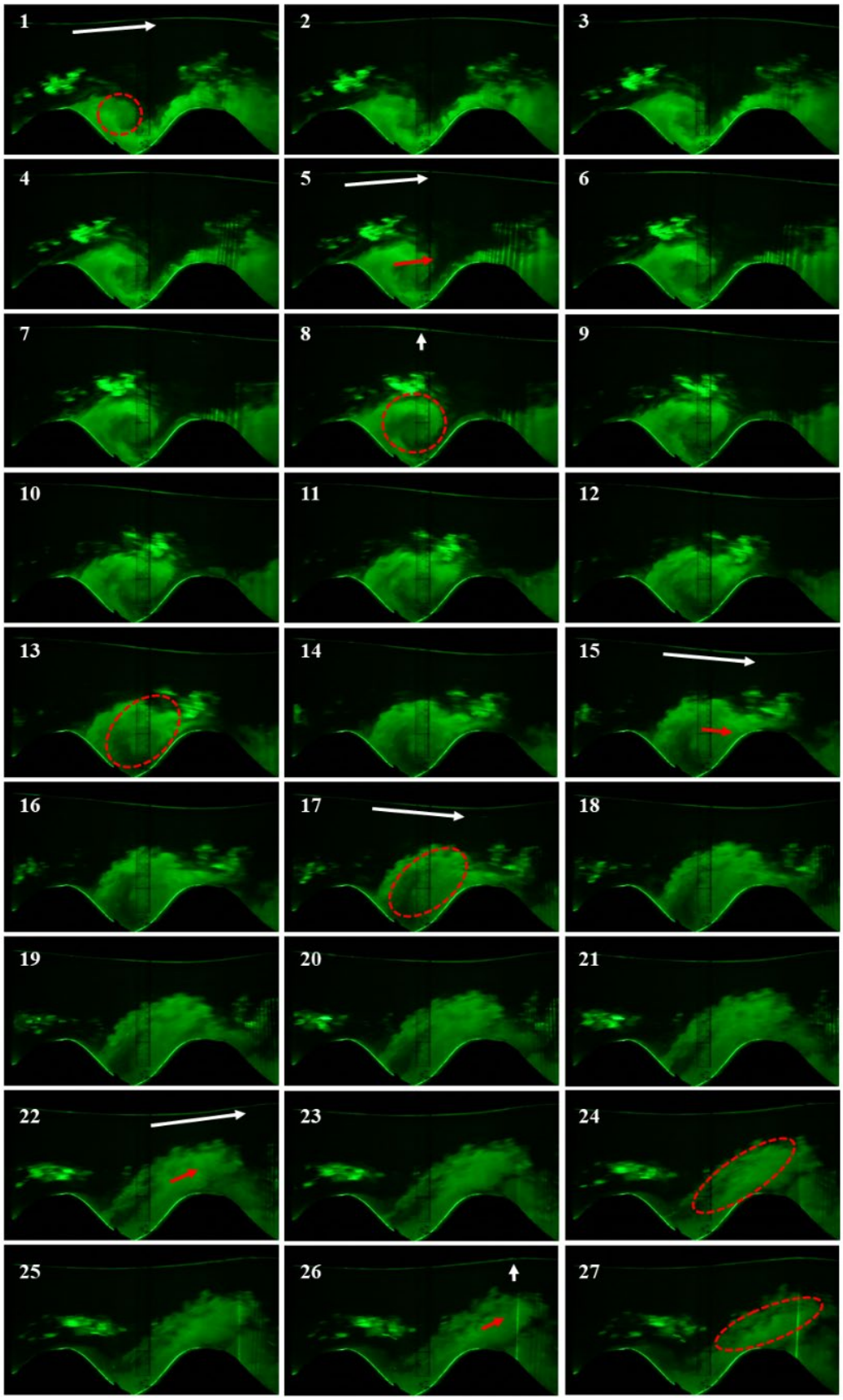

Figure 5. The overall motion process of the vortex water body observed through laser flow field tracing (with the bottom wave steepness of 0.333, the relative water depth of 0.8, and the Froude number of 0.24).

Potassium permanganate solution tracing of the flow field

Since during the flume experiment in the process of laser flow field tracing, the injection process of the tracer suspension was not stable, the laser flow field tracing was only aimed at observing the flow field characteristics above the rippled bottoms under the condition of the generation of upstream-propagating waves. However, the tracing with the saturated potassium permanganate solution, which injects the tracer solution evenly and slowly into the flow field through the dripping device, is more suitable for observing the flow field characteristics above the rippled patch under different flow velocity conditions (including the flow velocities when the upstream-propagating waves are generated and when waves do not appear). In this subsection, also based on the experimental conditions with the bottom wave steepness of 0.333 and the relative water depth of 0.8, three flow velocity conditions with Froude numbers of 0.17, 0.24, and 0.31 were set, corresponding respectively to the low flow velocity condition where no upstream-propagating waves were generated, the flow velocity condition where intensive upstream-propagating waves occurred, and the high flow velocity condition where no upstream-propagating waves were generated.

Tracing of the flow field characteristics under the low flow velocity condition where no upstream-propagating waves occur. Under the condition of low flow velocity (Froude number 0.17), no upstream-propagating waves appeared on the free water surface above the rippled bottoms. As can be seen from the continuous screenshots of the tracing video under this flow velocity condition (Fig. 6), there is a stable backflow area at the downstream position of wave crest #1 of the rippled patch. Although there are the backflow and rotation of water bodies at the rippled bottom's trough positions in Fig. 6, the flow characteristics of the backflow area always remain stable, and there is no periodic vortex shedding phenomenon.

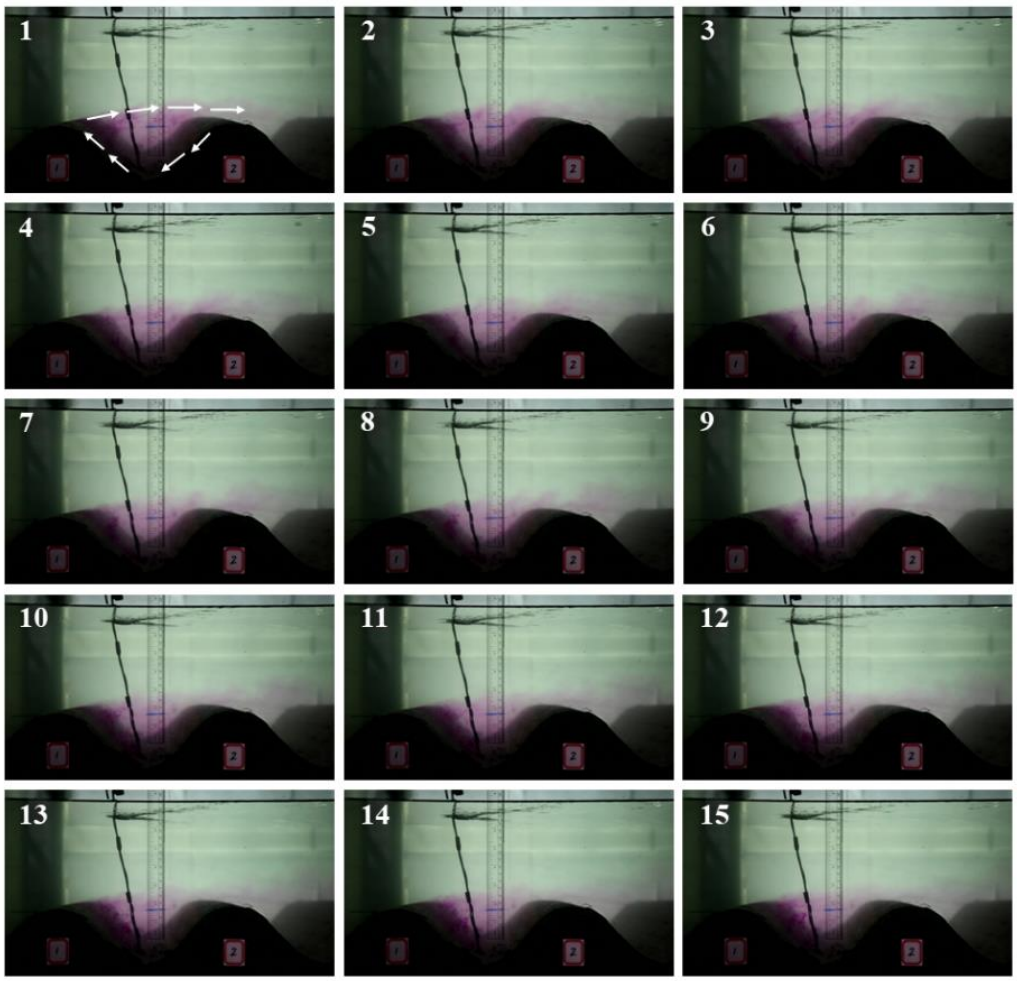

Figure 6. Potassium permanganate flow field tracing under the condition of low flow velocity (with no upstream-propagating waves appearing) (with the bottom wave steepness of 0.333, the relative water depth of 0.8, and the Froude number of 0.17).

Characteristics of flow field tracing under the condition of generating intensive upstream-propagating waves. Under the condition of the flow velocity (Froude number 0.24) that excites intensive upstream-propagating waves, violent fluctuations occur on the free water surface above the rippled patch, and obvious upstream-propagating waves are generated. As can be seen from the continuous screenshots of the tracing video under this flow velocity condition (Fig. 7), an obvious vortex structure appears above the troughs of the rippled bottoms, and the formation and motion processes of the vortex water body have obvious periodic characteristics, which are consistent with the observation results obtained through laser flow field tracing. Moreover, since the saturated potassium permanganate tracing solution is continuously released, through long-term flow field tracing, the periodic variation characteristics of the vortex water body caused by boundary layer separation on the downstream side of the rippled bottoms' crest can be identified more clearly.

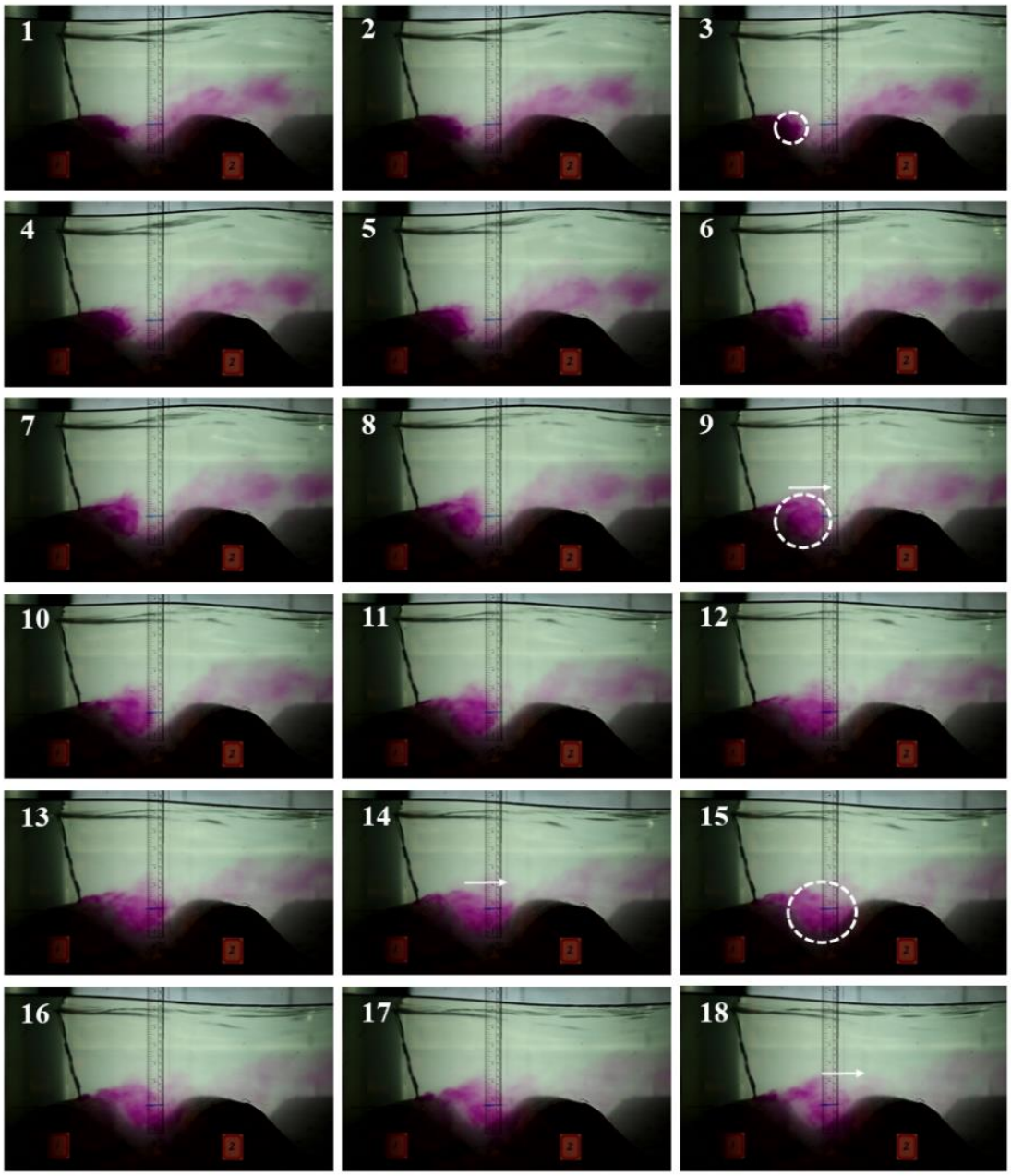

Figure 7. Potassium permanganate flow field tracing under the condition of the generation of upstream-propagating waves (with the bottom wave steepness of 0.333, the relative water depth of 0.8, and the Froude number of 0.24).

Characteristics of flow field tracing under the high flow velocity condition where no upstream-propagating waves appear. Under the condition of the experimental group with a high flow velocity (Froude number 0.31), no upstream-propagating waves were observed on the free water surface above the rippled bottoms, and only chaotic free-surface disturbances existed. As can be seen from the continuous screenshots of the tracing video under this flow velocity condition (Fig. 8), similar to the situation of the low flow velocity with a Froude number of 0.17, there is a stable backflow area at the trough position on the downstream side of the first rippled bottoms' crest. The backflow and rotation speeds of the vortex water body therein are faster, but there are no periodic characteristics. This indicates that when the water flow velocity is higher than the velocity range for exciting upstream-propagating waves, although the increase in the flow velocity enlarges the disturbances on the flow's free water surface, the phenomenon of periodic vortex generation and shedding no longer occurs.

Figure 8. Potassium permanganate flow field tracing under the high flow velocity condition (when the upstream-propagating waves disappear) (with the bottom wave steepness of 0.333, the relative water depth of 0.8, and the Froude number of 0.31).

CONCLUSIONS

The resonance among free-surface waves, ambient current, and rippled bottoms was investigated from the perspective of the tracing observation of flow field response under intensive resonance which is represented by the excitation of upstream-propagating waves.

Through the qualitative observations of flow field characteristics using the self-made laser sheet tracing method above the rippled bottoms at the excitation condition of upstream-propagating waves, the flow field between bottom wave crests was traced, which shows the details as vortex structure's

formation, growth, movement and deformation. There was backflow near the wall on the downstream side of the bottom crest and boundary layer separation. The motion of the vortex water body structure had periodicity related to water level changes at the free surface of the flow. Its overall motion is also related to water surface fluctuations.

Through the potassium permanganate solution flow field tracing carried out for the three flow velocity combinations with the bottom wave steepness of 0.333, the relative water depth of 0.8, and Froude numbers of 0.17, 0.24, and 0.31 respectively, the observation results show that the flow velocity condition for triggering the upstream-propagating waves has a significant correlation with the periodic shedding characteristics of the vortex structure in the backflow area on the downstream side of the sinusoidal rippled bottoms. Under the low and high flow velocity conditions where no upstream-propagating waves are generated on the water surface, the motion of the vortex water body in the backflow area always remains stable. Moreover, under the flow velocity condition for exciting the upstream-propagating waves, the vortex water body then presents the motion characteristics with the same frequency as the water surface fluctuations.

ACKNOWLEDGMENTS

This research was supported by the National Natural Science Foundation of China (Grant No. 52101308), the National Natural Science Foundation of China (Grant No. 52271271), and the Fundamental Research Funds for the Central Universities (Grant No. B240201012).

REFERENCES

Choi, W., Chabane, M., Taklo, T. 2021. Two-dimensional resonant triad interactions in a two-layer system, *Journal of Fluid Mechanics*, 907(A5), 1–41.

Davies, A.G., Heathershaw, A.D. 1984. Surface-wave propagation over sinusoidally varying topography, Journal of Fluid Mechanics, 144, 419-443.

Fan, J., Zheng, J.H., Tao, A.F., Gao, P., Li, S. 2014. Experimental study on critical resonant state of upstream-advancing waves, *Proceedings of 34th International Conference on Coastal Engineering*. 1(34), posters.11

Fan, J., Zheng, J.H., Tao, A.F., Yu, H.F., Wang, Y. 2016. Experimental study on upstream-advancing waves induced by currents, *Journal of Coastal Research*, 75, 846–850.

Fan, J., Zheng, J.H., Tao, A.F., Liu, Y.M. 2021. Upstream-propagating waves induced by steady current over a rippled bottom: Theory and experimental observation, *Journal of Fluid Mechanics*, 910(A49), 1–32.

Fan, J., Tao, A.F., Zheng, J.H., Peng, J. 2022. Numerical investigation on temporal evolution behavior for triad resonant interaction induced by steady free-surface flow over rippled bottoms. *Journal of Marine Science and Engineering*, 10(1372), 1–15.

Kennedy, J.F. 1963. The mechanics of dunes and antidunes in erodible-bed channels, *Journal of Fluid Mechanics*, 16(04), 521-544.

Kyotoh, H., Fukushima, M. 1997. Upstream-advancing waves generated by a current over a sinusoidal bed, *Fluid Dynamics Research*, 21, 1–28.

Liu, Y., Yue, D. K. P. 1998. On generalized Bragg scattering of surface waves by bottom ripples, *Journal of Fluid Mechanics*, 356, 297–326.

McHugh, J.P. 1992. The stability of capillary-gravity waves on flow over a wavy bottom, *Wave Motion*, 16(1), 23-31.

Mei, C.C. 1969. Steady free surface flow over wavy bed, *Journal of the Engineering Mechanics Division*, 95(6), 1393-1402.

Mei, C. C. 1985. Resonant reflection of surface water waves by periodic sandbars, *Journal of Fluid Mechanics*, 152, 315–335.

Mei, C.C, Stiassnie, M., Yue, D.K.P. 2005. *Theory and Applications of Ocean Surface Waves: Linear Aspects*, World Scientific, Singapore, 307-323.

Mizumura, K. 1995. Free-surface profile of open-channel flow with wavy boundary, *Journal of Hydraulic Engineering*, 121(7), 533-539.

Raj, R., Guha, A. 2019. On Bragg Resonances and Wave Triad Interactions in Two-Layered Shear Flows. *Journal of Fluid Mechanics*, 867, 482–515.

Yih, C. S. 1976. Instability of surface and internal waves, *Advances in Applied Mechanics*, 16, 369–419.